Sensor Applications

Remote Heart Rate Estimation of Canines using a mmWave Radar and Depth Camera

Nicholas Bowden[1], Robert Gillette[2], Stephen Paine[1*], and Amir Patel[1,3**]
[1]Department of Electrical Engineering, University of Cape Town, South Africa, [2]Sportsvet Inc, Lancaster, SC, USA, [3]Department of Computer Science, University College London, London, UK.
[*]Member, IEEE, [**]Senior Member, IEEE

Manuscript received.

Abstract—While heart rate estimation with Frequency Modulated Continuous Wave (FMCW) radar on humans has become a common research topic, the potential of this technology for vital sign monitoring of animals such as canines has had little exploration. This paper serves as a study on the feasibility of applying mm-wave FMCW heart rate estimation technology on conscious canines. A data capture system and remote heart rate estimation pipeline is implemented and used on canine subjects. Several methods are compared which include peak counting, spectrogram analysis, Long-Short Term Memory (LSTM) Neural Networks and a Hybrid Digital Signals Processing (DSP)-LSTM Approach. While the dogs were not stationary enough for traditional DSP approaches to produce meaningful results, the Hyrbid DSP-LSTM approach improved the overall accuracy (13.9 RMSE bpm and a 0.76 Correlation Coefficient). These improvements will greatly increase the feasibility of mm-wave technology for future applications in livestock monitoring and wildlife conservation.

Index Terms—remote vital signs monitoring, heart rate estimation, canine vital signs, FMCW, ROS2

I. INTRODUCTION

Heart rate is an important physiological indicator of health which has has resulted in FMCW radar being frequently explored as a tool for remote health monitoring in humans [1]. Domestic canines share close spaces with humans which leads to transference of zoonotic diseases between humans and canines. Therefore, monitoring both human and canine heart rates could provide key insights that could keep both species healthy [2].

Heart rate monitoring with FMCW radar measures very small movements of the skin caused by cardiac and respiratory activity to estimate heart-rate. These fine displacements can be encoded into the phase of successive radar chirps [1]. Displacements in the skin caused by cardiac and respiratory activity are not limited to humans but can be found in any animal, including dogs. Therefore, the same principle applied to humans should be transferable to canines. However, heart rate estimation with FMCW radar has one caveat which is that it requires the participant to remain exceptionally still which may not be possible when trying to measure the heart rate of awake canines [9].

This paper presents a study of the feasibility of FMCW heart rate estimation on canines. Impulse Radio - Ultra Wide Band (IR-UBW) radar has been used by Wang *et al.* [2], [3] for measuring the heart rate of sleeping canines, suggesting radar is suitable for canine heart rate estimation. Additionally, this paper combines time-synchronised data from several sources to automate the data collection process in a flexible way such that data generated by our system can be used for multiple applications beyond heart rate estimation.

Corresponding author: N. Bowden (e-mail: bwdnic001@myuct.ac.za).
Associate Editor: XXX.
Digital Object Identifier:

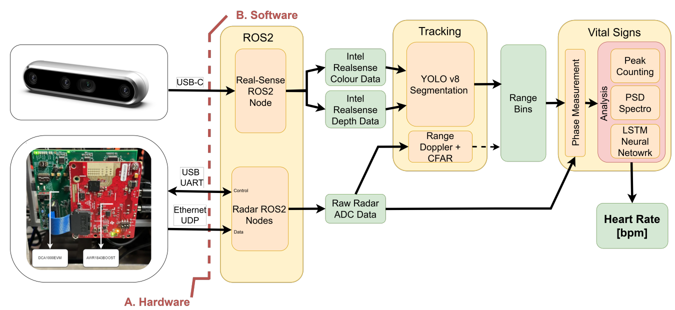

Fig. 1: Diagram of system overview moving from hardware through recording with ROS2, tracking and finally vital sign measurement.

This paper begins with short description of the system used to generate the data in Section II which includes overviews of both the hardware and software. Section III explains the methods used for radar range bin selection which include basic radar DSP techniques and the usage of a zero shot neural network and a stereo depth camera to visually determine the range bin. Section IV discusses how the heart rate is calculated. In Section V we present our methodology and corresponding results and discussion.

II. DATA CAPTURE SYSTEM

A. Hardware

Three key pieces of hardware were used to collect the data from the dogs examined in this study as shown in Fig. 1. First, a Polar H10 heart rate belt was used to capture ground truth data from the dog to validate our pipeline. The feasibility of the Polar H10 belt for successful canine heart rate measurement was confirmed by Worakan *et al.* [4]. Second, the radar used was a Texas Instruments

(TI) AWR1843Boost system which was accompanied with a TI DCA1000EVM for raw ADC data capture. The parameters of the radar are shown in Table 1. Third, an Intel Real-Sense stereo camera was added as an additional means of range-bin selection as the camera is capable of producing depth measurements as well as colour images.

Table 1: Radar Chirp Parameters

Parameter Name	Value
Number of Samples	96
Sample Rate [Ksps]	2200
Sweep Rate [MHz/μs]	70
Starting Frequency [GHz]	77
Number of Chirps	32
Idle Time [μs]	100
Ramp Time [μs]	57.14
Frame Period [ms]	15.3

B. Software

This section explains how the three components in Fig.1 were integrated using ROS2 to produce timestamped data. Each device ran its own ROS2 nodal network. The Intel RealSense camera had an existing ROS2 driver providing color/depth images and extrinsic parameters. The TI radar lacked a ROS2 driver for raw ADC data, so a back-end ROS2 server handled control while another node captured ADC packets. CLI-accessible front-end nodes performed radar configuration and provided start and stop recording functionality. Finally, a custom ROS2 driver connected the Polar H10 via Bluetooth for heart-rate data.

The enhanced Communication Abstraction Layer (eCAL), a DDS, stored all ROS2 messages as serialized bytes, improving performance but requiring subsequent deserialization. Radar data arrived as interleaved bytes, so a sorting algorithm (based on TI documentation) created a radar data cube. After deserialization and sorting, the data entered the Tracking and Vital Signs Pipeline (Sections III–IV).

III. TRACKING PIPELINE

The tracking part of the overall pipeline, shown in Fig. 1, is used to determine the radar range bin of the target. The range bin is required for the phase measurement process because the algorithm needs to know which slice of range bins to select In-Phase and Quadrature (IQ) samples from. In this paper we explore two possible pipelines for target tracking that could be used together or separately.

A. Radar Tracking

The radar only pipeline uses traditional FMCW techniques to determine the target position. The first step involved applying successive Fast Fourier Transforms (FFTs) to the radar data cube to generate an Amplitude Range-Doppler (ARD) map. This is followed by the application of a Constant False Alarm Rate (CFAR) algorithm to pull detections from the ARD map [7], thus allowing the dog and handler to be detected separately.

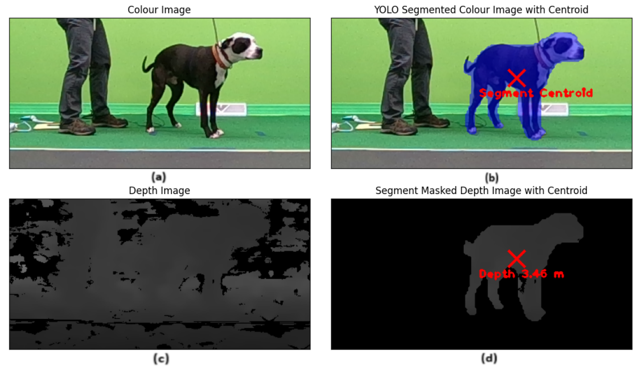

Fig. 2: Intel Real-Sense Stereo Camera tracking canine tracking outputs using YOLO v8 instance segmentation. **(a)**: The original colour image. **(b)**: Colour image after segmentation with YOLO. **(c)**: Original depth image. **(d)**: Depth image masked with segmentation overlay.

B. Stereo Camera Tracking

The Intel RealSense uses two IR cameras for depth imaging (Fig.2,(c)), enabling 3D dog tracking via known camera extrinsics. It also includes an RGB camera (Fig.2,(a)). Continuous range measurements automatically selected the correct chest range bin, even as the dog moved. Corresponding phase changes in neighbouring bins further eased the selection. A pre-trained YOLO network [5] isolated the dog's pixels via instance segmentation (Fig.2,(b)). After aligning depth and colour images, these pixels masked the depth image (Fig.2,(d)). The dog's centroid was then computed to locate the chest and its range bin.

IV. VITAL SIGN PIPELINE

A. Phase Measurement

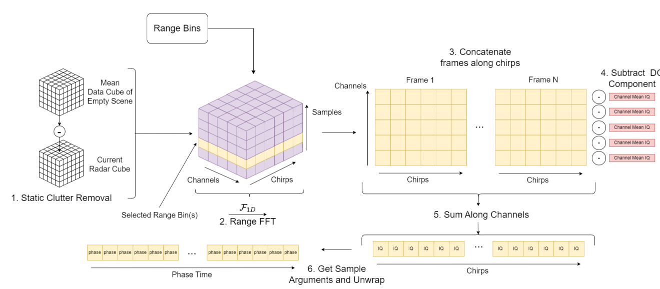

Fig. 3: Diagram of the phase measurement process performed by the system.

The phase measurement process is explained in Fig. 3 and involves several steps. The first two steps shown in Fig. 3 are actually the first two steps of the ARD process. The clutter removal is not necessary but is kept for efficiency as the range FFT is required. Therefore the steps required to compute the phase measurement include performing the range FFT, range bin selection, chirp concatenation, IQ DC offset compensation, coherent channel summation and phase arc-tangent demodulation and unwrapping.

Once the phase-time signal was created it could be filtered to isolate the heart rate signal.

B. Filtering

An Infinite Impulse Response (IIR) Butterworth filter was used due to its flat pass band which prevented any distortion of the heart rate signal. The filter used in this paper was implemented with SciPy's *sosFiltFilt* function [8]. This function takes in the unfiltered signal and a Second Order Sections (SOS) implementation of a desired filter and runs the filter over the signal forwards and backwards. This doubles the order of the filter and eliminates any phase shift caused by the filter. Thus, even though the filter used was non-linear, the application of the filter forwards and backwards ensures the signal is undistorted at the cost of the filter becoming non-causal and only suitable for block processing.

C. Heart Rate Estimation

After the heart rate band was isolated, four methods were used to calculate the heart rate. These included Peak Counting, Spectrogram Analysis, a LSTM Neural Network and a Hybrid LSTM Network Approach.

1) Peak Counting: Peaks were found by finding the local maxima within the filtered phase-time signal. The index of each peak was used to locate the time value of where the peak occurred. Taking the difference between each time value found yielded the time between peaks which effectively is the Inter-Beat Interval (IBI), T_{ibi}, used to calculate heart rate. The heart rate is calculated by dividing 60 by T_{ibi} which is then passed through a moving average filter.

2) Normalised PSD Spectrogram: Power Spectral Density (PSD) Spectrograms on time series data are performed by repeatedly selecting data using a sliding window and performing FFTs on the overlapping selected data. Each FFT forms a single column on the spectrogram image. Columns are concatenated together to form a 2D image with frequency on the Y axis and time on the X axis. The magnitude of the coefficients of each FFT are squared and scaled to get the PSD. This forms a visual representation of how the frequency components change over time. The columns of the spectrogram are then normalised to the frequency with the highest signal strength which is assumed to be the heart rate.

3) LSTM Neural Network: LSTM networks are widely used for time-series classification [1]. Zhao *et al.* [1] preferred a 1D CNN over an LSTM due to real-time speed constraints, but our post-processed data made LSTM feasible. We used an LSTM layer with 32 hidden units, followed by fully connected layers of sizes 64, 32, 16, and 1. The input was a 10-second (310-sample) block of unwrapped, filtered phase data, labeled with the mean Polar H10 heart rate for that time window. We split the dog phase data into 80% training, 10% validation, and 10% testing, then used the model with the lowest validation loss for final predictions. Due to limited data, the same dogs appeared in training and testing, but with distinct sample sets.

4) Hybrid Approach: In a paper by Bauersfeld *et al.* [11], the authors combine traditional and deep learning (DL) approaches to improve the model of a quad-copter. They train their network to output the errors between the model-based method and the measured values they try to estimate. This incorporates more information into their measurements which produces a better result. This is similar to the Kalman filter philosophy which proposes that one should never throw away any information [12].

A similar approach as shown in Fig. 4 was attempted by training the same LSTM used in the LSTM only approach to output the error

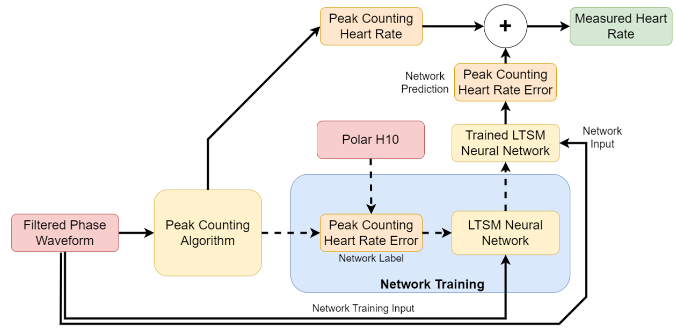

Fig. 4: Diagram of data processing algorithm for the Hybrid LSTM Approach

of the peak counting algorithm. The predicted error is then added onto the value of the peak counting algorithm in an attempt to correct the final value created by the algorithm.

V. EXPERIMENTS AND RESULTS

A. Methodology

Each dog was placed in front of the radar-camera assembly with the Polar H10 strapped around the chest[1]. The handler was told to stay behind the dog so that the handler could be filtered out during the range bin selection process. Recordings were done in 30 s sessions with the dog remaining as still as possible during the recording. Four different dogs were separately recorded at several ranges and angles.

B. Results

This section presents the statistical results of different methods shown in Table 2 as well as an example output of the best performing approach (the Hybrid LSTM) as shown in Fig. 5.

Table 2: Table of statistical results for canine heart rate estimation.

Metrics	Peak Counting	Spectrogram	LTSM Network	Hybrid Approach
Accuracy [%]	78.2 ± 11.0	73.2 ± 12.4	84.7 ± 13.1	88.2 ± 7.55
RMSE [bpm]	23.4	30.7	19.6	13.9
Pearson Coefficient	0.010	0.020	0.45	0.76

C. Discussion

Conventional methods such as peak counting and spectrogram frequency analysis boast a fairly high accuracy, above 70 %. However, the Root Mean Square Error (RMSE) shows a different perspective. The pipeline produces very high errors, well over 20 bpm. This is confirmed by the Pearson Coefficient for these methods which show no correlation with the data. This highlights the importance of choosing suitable performance metrics.

The pipeline and system used in this paper were previously validated on exceptionally still humans with excellent results that had very low RMS errors. However, it is important to note that the papers by Wang

[1]This study was approved by the University of Cape Town, Science Faculty Animal Ethics Committee (ref: 2023/V4/AP/A)

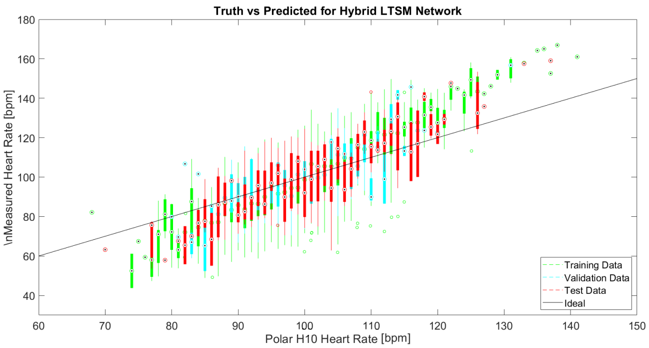

Fig. 5: A box and whisker plot of the results for the Hybrid LSTM Aproach for training, validation and test data

et al. [2], [3] dealt with sleeping animals. Signal degradation due to movement by awake canines was reported in a paper by Amano *et al.* [13]. These movements, termed random body motion (RBM) in a review paper by Gouveia *et al.* [10], are a known issue with radar based heart rate estimation and are the clear cause of the errors seen in this paper for the traditional DSP approaches as seen in the paper by Amano *et al.* [13].

While the traditional DSP approaches did not seem to produce meaningful results, some promise was shown using the LSTM Network with slight improvements in RMSE and the Correlation Coefficient. Adapting the work of Bauersfeld *et al.* [11], the Hybrid approach shows a much higher correlation and accuracy and much lower RMSE. With more data and further research, it could be possible to optimise this approach to produce very accurate and precise results.

VI. CONCLUSION

A system and pipeline were designed from scratch to measure the heart rate of canines remotely after being validated on humans. Awake and active canines caused too much RMB for traditional DSP methods to measure heart rate accurately. While the results seem to point to a high accuracy, the Pearson Coefficient shows no correlation between the ground truth and calculated results, highlighting the importance of good performance metric choice. Using an LSTM network yielded better results but were still not entirely satisfactory. Building on the work in the paper by Bauersfeld *et al.* [11], a Hybrid LSTM Approach was attempted that greatly improved results. Table 3 draws comparisons with previous works to highlight the novelties in our approach.

Table 3: Comparison to Previous Work

Paper	Comparison and Key Differences
[1]	Uses ML (fully connected NN) to extract heart rate from the ankle of stationary humans with an FMCW radar. In contrast, we apply a **hybrid DSP+ML** approach to handle the **RMB issue** in awake canines, incorporating ML to refine DSP outputs.
[3]	Focuses on **sleeping** canines and cats using ultra-wideband radar and pure DSP (filters, VMD, FFT). Our work extends to **awake** animals and compares DSP- vs ML-based methods to show performance benefits of ML.
[13]	Studies sleeping and awake canines at up to 1 m, noting signal degradation in awake subjects but not resolving it. We directly address this limitation via a **novel hybrid DSP+ML** method to tackle awake canines' RMB problem.

Future research concerning remote canine vital signs should focus on the use of machine learning and hybrid machine learning models to get better results. Furthermore, additional improvements can be made to the ML training process by significantly increasing the sample size of the data collected and ensuring that completely separate sets of canines are used for training and testing. Additionally, in future work it would be beneficial to properly combine both camera and radar tracking measurements to provide additional RBM compensation before the input to the Hybrid Approach.

ACKNOWLEDGMENT

We would like to extend a heartfelt thanks to Jeannie Willems from Nutramax Wellness and Performance Center for her help during this research project. Additionally, we like to thank Nutramax Laboratories for their support and the use of their facilities during the data capture phase of this paper.

REFERENCES

[1] Zhao, Peijun, Chris Xiaoxuan Lu, Bing Wang, Changhao Chen, Linhai Xie, Mengyu Wang, Niki Trigoni, and Andrew Markham. 'Heart Rate Sensing with a Robot Mounted mmWave Radar'. In 2020 IEEE International Conference on Robotics and Automation (ICRA), 2812–18. Paris, France: IEEE, 2020. https://doi.org/10.1109/ICRA40945.2020.9197437.

[2] Wang P, Zhang Y, Ma Y, Liang F, An Q, Xue H, Yu X, Lv H, Wang J. Method for Distinguishing Humans and Animals in Vital Signs Monitoring Using IR-UWB Radar. Int J Environ Res Public Health. 2019 Nov 13;16(22):4462. doi: 10.3390/ijerph16224462. PMID: 31766272; PMCID: PMC6888617.

[3] Wang, Pengfei, Yangyang Ma, Fulai Liang, Yang Zhang, Xiao Yu, Zhao Li, Qiang An, Hao Lv, and Jianqi Wang. 2020. "Non-Contact Vital Signs Monitoring of Dog and Cat Using a UWB Radar" Animals 10, no. 2: 205. https://doi.org/10.3390/ani10020205.

[4] Worakan Boonhoh and Tuempong Wongtawan. 'The Application of Human Heart Rate Monitor in Dogs: A Preliminary Study', 2022. https://doi.org/10.13140/RG.2.2.24896.00007.

[5] Redmon, Joseph, Santosh Divvala, Ross Girshick, and Ali Farhadi. 'You Only Look Once: Unified, Real-Time Object Detection'. arXiv, 9 May 2016. http://arxiv.org/abs/1506.02640.

[6] Texas Instruments. 'Mmwave Radar Device ADC Raw Data Capture', 2018. https://www.ti.com/lit/an/swra581b/swra581b.pdf?ts=1707049781615: :text=The %20DCA1000%20captured%20data%20samples,LVDS%20lane%20will%20be %20stored.

[7] Vally, Azraa, Nicholas Bowden, Lindelani Mbatha, Gerald Maswoswere, Stephen Paine, Paul Amayo, Andrew Markham, and Amir Patel. 'M2S2: A Multi-Modal Sensor System for Remote Animal Motion Capture in the Wild', n.d.

[8] Pauli Virtanen, Ralf Gommers, Travis E. Oliphant, Matt Haberland, Tyler Reddy, David Cournapeau, Evgeni Burovski, Pearu Peterson, Warren Weckesser, Jonathan Bright, Stéfan J. van der Walt, Matthew Brett, Joshua Wilson, K. Jarrod Millman, Nikolay Mayorov, Andrew R. J. Nelson, Eric Jones, Robert Kern, Eric Larson, CJ Carey, İlhan Polat, Yu Feng, Eric W. Moore, Jake VanderPlas, Denis Laxalde, Josef Perktold, Robert Cimrman, Ian Henriksen, E.A. Quintero, Charles R Harris, Anne M. Archibald, Antônio H. Ribeiro, Fabian Pedregosa, Paul van Mulbregt, and SciPy 1.0 Contributors. (2020) SciPy 1.0: Fundamental Algorithms for Scientific Computing in Python. Nature Methods, 17(3), 261-272.

[9] Lv, Wenjie, Wangdong He, Xipeng Lin, and Jungang Miao. 'Non-Contact Monitoring of Human Vital Signs Using FMCW Millimeter Wave Radar in the 120 GHz Band'. Sensors 21, no. 8 (13 April 2021): 2732. https://doi.org/10.3390/s21082732.

[10] Gouveia C, Vieira J, Pinho P. A Review on Methods for Random Motion Detection and Compensation in Bio-Radar Systems. Sensors (Basel). 2019 Jan 31;19(3):604. doi: 10.3390/s19030604. PMID: 30709017; PMCID: PMC6387256.

[11] Bauersfeld*, Leonard, Elia Kaufmann*, Philipp Foehn, Sihao Sun, and Davide Scaramuzza. 'NeuroBEM: Hybrid Aerodynamic Quadrotor Model'. In Robotics: Science and Systems XVII. Robotics: Science and Systems Foundation, 2021. https://doi.org/10.15607/RSS.2021.XVII.042

[12] Pei, Yan, Swarnendu Biswas, Donald S. Fussell, and Keshav Pingali. 'An Elementary Introduction to Kalman Filtering'. arXiv, 27 June 2019. http://arxiv.org/abs/1710.04055.

[13] Rina Amano. 'FMCW Radar-Based Monitoring of Canine Vital Signs Validated Using IMU'. March 2024. https://cir.nii.ac.jp/crid/1390863937794512384